

AD-A102 550

MCDONNELL DOUGLAS ASTRONAUTICS CO HUNTINGTON BEACH CA

F/G 4/1

ELECTRIC FIELDS IN EARTH ORBITAL SPACE.(U)

JUN 81 W P OLSON, K A PFITZER, W J SCOTT

N00014-80-C-0796

UNCLASSIFIED

MDC-69606

NL

1 of 1
AD A
102 550

END
DATE
FILMED
8-81
DTIC

LEVEL

12

AD 100550

DTIC

AUG 7 1981

30 2214 02 (08 JAN 70)

DTIC FILE COPY

MCDONNELL DOUGLAS ASTRONAUTICS COMPANY

MCDONNELL DOUGLAS

CORPORATION

DISTRIBUTION STATEMENT A

Approved for public release;
Distribution unlimited

06 040

**MCDONNELL
DOUGLAS**
CORPORATION

(11) JUNE 1981

(6) ELECTRIC FIELDS IN EARTH ORBITAL SPACE

(9) FINAL REPORT

(13) CONTRACT NO. 0014-80-C-0796

(14) MDC-G9606

(12) 39

by 10

Principal Investigator: W. P. Olson

Co-Investigators: K. A. Pfitzer
W. J. Scotti

DTIC

AUG 7 1981

Sponsored by
Office of Naval Research
Washington, D.C. 20350

DISTRIBUTION STATEMENT A
Approved for public release;
Distribution Unlimited

MCDONNELL DOUGLAS ASTRONAUTICS COMPANY-HUNTINGTON BEACH

5301 Bolsa Avenue Huntington Beach, California 92647 (714) 896-3311

379320

TABLE OF CONTENTS

	<u>PAGE</u>
Section 1 - INTRODUCTION AND SUMMARY OF WORK	1
Section 2 - THE ENTRY OF LOW ENERGY PARTICLES INTO THE MAGNETOSPHERE.	4
Section 3 - THE LOCAL ACCELERATION OF CHARGED PARTICLES IN THE INNER MAGNETOSPHERE	18
Section 4 - LIST OF PRESENTATIONS AND PUBLICATIONS	34

Accession For	
NTIS GSA&I	<input checked="" type="checkbox"/>
DTIC TAB	<input type="checkbox"/>
Unannounced	<input type="checkbox"/>
Justification	<i>Per</i>
<i>on file</i>	
By	
Distribution/	
Availability Codes	
Dist	Avail and/or Special
<i>A</i>	

Section 1

INTRODUCTION AND SUMMARY OF WORK

In this report we discuss work performed during the past year on Contract No. N00014-80-C-0796. Two general areas of research were examined; one on the entry of charged particles into the earth's magnetosphere, the other on the local acceleration of charged particles in the inner magnetosphere.

Our early work with ONR support was focused on defining electric fields in the earth's magnetosphere. At an early date it was realized that in order to do this, it was first necessary to accurately describe the magnetospheric magnetic field. This led to the development of quantitative models of the earth's magnetospheric magnetic field and the study of its interaction with energetic charged particles (solar cosmic rays). It has only been in the past two or three years that the magnetic field models have been developed to the point that we could finally pose quantitative questions concerning the generation and maintenance of the electric fields in the earth's magnetosphere. About three years ago, we requested and received from ONR support to examine those electric fields induced by time variations in the magnetospheric magnetic field. It was felt that we could look at these fields quantitatively because, by that time, we had a good knowledge of the magnetospheric magnetic field and how it is influenced by temporal variations in the major magnetospheric current systems. This study of induced electric fields has led us to routinely determine not only the magnetic field, but also the magnetic vector potential for each new magnetic field model we develop. This is because the time variation in the magnetic vector potential leads directly to the induced electric field caused by temporal variations in the magnetic field.

We realized that having the primary induced electric field was not sufficient because the magnetospheric plasma responds to its presence. Charged particles in the magnetosphere are influenced by the total electric field resulting from the primary source (caused by temporal variations in the magnetic field), and a secondary source (caused by the response of the magnetospheric plasma to the initial induced electric field).

When these field models were first used to study the energization of charged particles in the earth's magnetosphere, it was found that computer costs for such studies were prohibitive. Thus in the past year, we were forced to develop procedures for representing the magnetospheric magnetic and induced electric fields in the inner magnetosphere that are very efficient computer-wise. This involved the use of Euler potentials, which permitted us to get rid of one of the integration subroutines which calls our magnetic fields subroutines frequently (needed for the determination of total electric field). The interesting results of this study (which has been a theme throughout our work with ONR) are discussed in Section 3 on particle energization.

We are now attempting to generalize the use of Euler potentials to the magnetospheric tail field with the hope that we can examine both magnetic and electric fields present in the tail of the earth's magnetosphere during substorms and be able to study the dynamics of charged particles and in plasmas in the earth's tail during these disturbed magnetic periods.

By 1979 we had quantitatively modeled the magnetospheric magnetic field and the induced electric field. However, there remains the electrostatic field in the earth's magnetosphere which persists predominantly in the tail region. This led us in the past year to reexamine our understanding of the entry of charged particles into the earth's magnetosphere. Traditionally, the magnetospheric field topology is described as either "open" or "closed". An open magnetosphere has some magnetic field lines connected to the interplanetary field, whereas a closed magnetosphere has no magnetic field lines penetrating its boundary, the magnetopause. In a closed magnetic field topology, it has been generally assumed that low energy particles cannot gain entry. This is largely because of the classical description of pressure balance which assumes that particles are specularly reflected over the entire magnetosphere. (The pressure balance equation states that the magnetopause will be found where the kinetic pressure of the solar wind balances the energy density (pressure) of the geomagnetic field. This equation has been used to theoretically determine the shape and size of the magnetosphere.) The assumption of specular reflection implies that the magnetic field at the magnetopause (at the point of reflection) is uniform and as a charged particle enters the magnetospheric magnetic field region it sees a uniform magnetic

field and the trajectory it traverses is a portion of a circle. However, in the real magnetosphere, there are gradients in the magnetic field along the magnetopause. This suggests that the particle's trajectory in the magnetospheric magnetic field region is noncircular. It is then possible that some of the particles incident on the magnetopause may actually gain entry to the magnetosphere, even in this "closed" magnetic field topology.

As usual, we have examined the problem quantitatively. We have looked at charged particles of varying energies, impacting the magnetopause at different angles and asked whether or not they can remain in the magnetosphere. We have found that along the flanks of the tail a very large number of incident particles actually gained entry to the magnetosphere when we drop the assumption of pressure balance and use the more realistic magnetospheric magnetic field which includes gradients parallel to the magnetopause. We believe that this particle entry is important for many magnetospheric processes. We have found that the particles enter near the equatorial region of the tail, suggesting that they may play a large role in forming and maintaining the plasma sheet. It is also clear that the old pressure balance formalism must be made more accurate by taking into account the presence of some entering charged particles. It is expected that this will make the nose of the magnetosphere more blunt and cause the tail field to have more flare. Both of these alterations to previous theoretical shapes will bring the new shape into much better agreement with observed magnetopause topology.

Our main concern, however, is with the electrostatic field in the tail. We believe that the close examination of the microphysics of the magnetopause, including this work on realistic particle entry, should shed light on mechanisms that may cause and maintain charge separation along the flanks of the tail of the magnetosphere. It is with this ultimate question in mind that we are proceeding to examine particle entry. It is hoped that we will eventually be able to quantitatively understand the formation and maintenance of electrostatic fields in the tail of the magnetosphere. With the electrostatic field and our quantitative understanding of induced electric fields, we will then have a fairly complete picture of the electromagnetic field in the magnetosphere and be able to discuss quantitatively and realistically the motions of plasmas and low energy charged particles in the earth's magnetosphere.

Section 2

THE ENTRY OF LOW ENERGY PARTICLES INTO THE MAGNETOSPHERE

Magnetospheric magnetic field models have traditionally been developed using a pressure balance formalism in which the solar wind particles are assumed to be specularly reflected by the earth's magnetic field. That is, the angle the particle makes to the vector normal to the surface is the same as it approaches and after reflection. This formalism therefore assumes the magnetic field is constant in the vicinity of the reflection region. This formalism gives rise to a magnetic field that is confined to a limited region space. The magnetospheric magnetic field thus developed is "closed", i.e., no field lines penetrate through the boundary between the magnetosphere and the shocked solar wind (the magnetopause).

Although such field topologies are magnetically closed, they are not closed to the entry of charged particles. Work on cosmic rays several years ago by our group illustrated that energetic charged particles had ready access to a closed magnetosphere and can propagate to almost any point within it. In the past year, in an attempt to ask questions concerning the formation of electrostatic fields in the tail of the magnetosphere, we have found it necessary first to examine the question of entry of low energy particles into a closed magnetosphere. We have found that charged particles can easily enter the flanks of the magnetospheric tail and then flow across the tail to form and maintain at least a part of the plasma sheet. We intend to examine particle entry over the entire magnetopause but have, to date, examined only the tail region in detail.

ENTRY INTO A MAGNETICALLY CLOSED REGION

Figure 1 schematically shows how particles are able to enter into a magnetically closed region. Whenever a magnetic field has gradients parallel to the boundary, a particle entering the magnetic field will begin to gradient drift. It is this fact that the real magnetospheric field possesses gradients parallel to the magnetopause that permits particle entry. In the pressure balance

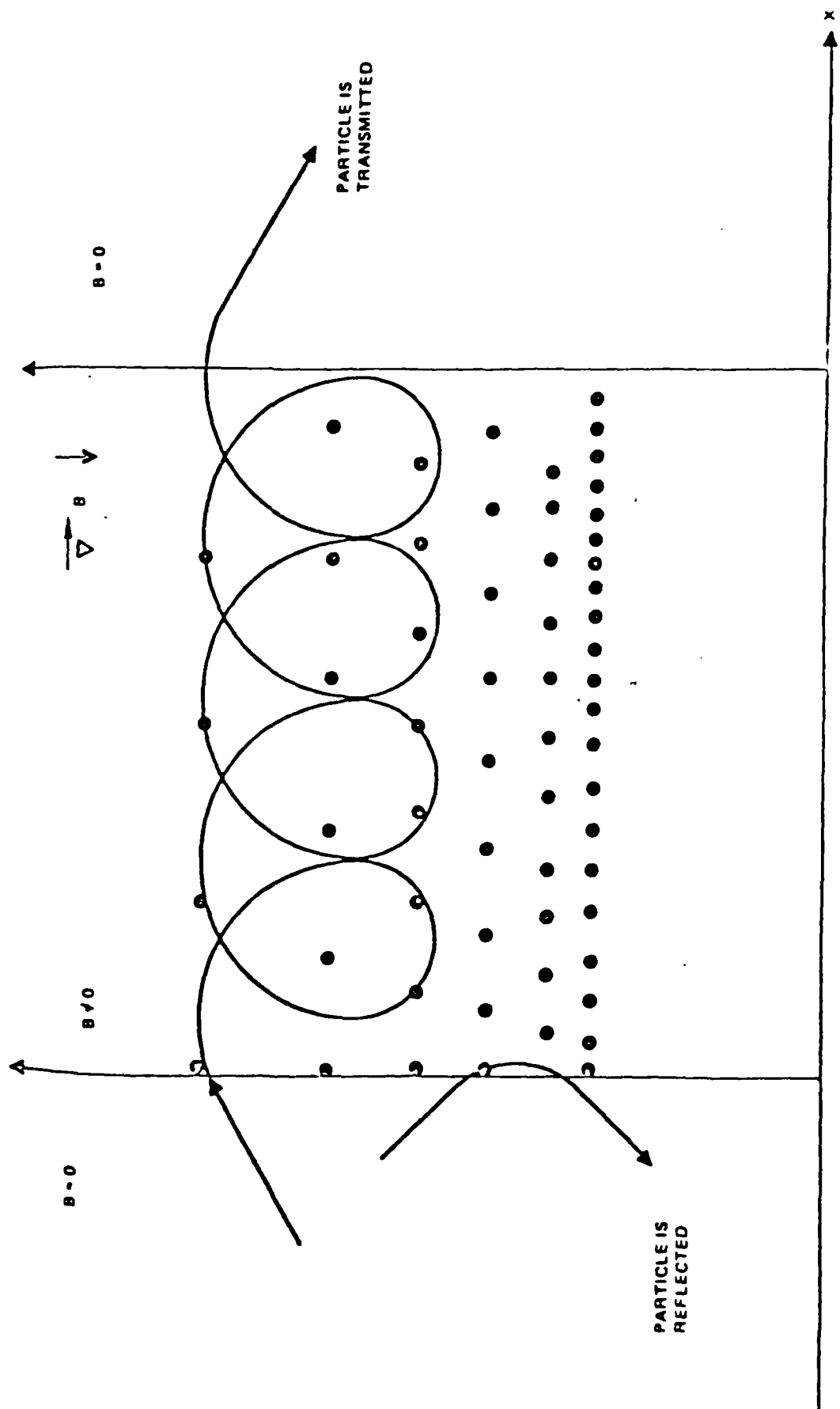


Figure 1. Particle reflection by or transmission through a non-uniform magnetic field

formalism, specular reflection implies that the field is uniform in the region where the particle is being reflected so that while the particle is in the magnetosphere, its trajectory is exactly circular. Thus every particle that enters through a "mathematically thin" magnetopause to be influenced by the geomagnetic field will, in less than one gyrocircle, exit the magnetosphere. When the more realistic representation of the magnetospheric magnetic field is used which includes gradients in the field in the region where the particle is incident, then it is possible for particles to remain in the magnetosphere once their trajectories have carried them through the magnetopause.

There exists a range of "impact angles" over which particles can enter the field region. If the magnetic field region is of finite extent, the particle will later exit the field region and return to infinity as specified by Louiville's theorem. Thus, in the case of the magnetospheric tail, protons can enter on the dawn side, drift through the tail and exit on the dusk side. Electrons enter the dusk side and exit at dawn.

CONSTRUCTION OF A MAGNETICALLY CLOSED REGION

A magnetically closed magnetosphere was defined using our 1974 magnetic field model. The study was limited to an X_{SM} of -20 to $-40 R_E$. In this region the magnetic field model has a well behaved tail with no wandering field lines. The boundary was defined by first drawing a circle of $18 R_E$ radius in the $X_{SM} = -10 R_E$ plane with a center on the X_{SM} axis. The field lines which pass through this circle were defined as boundary lines (see Figure 2). The field was thus defined as identically zero outside the boundary and equivalent to the 1974 model values everywhere inside of the boundary. At the boundary the magnetospheric field lines are everywhere parallel to the boundary.

ENTRY CALCULATIONS

Proton entry efficiencies into this magnetically closed magnetosphere were determined using numerical techniques. Test particle trajectories at different locations, different energies and various impact angles were integrated using the Lorentz force equation. The protons were allowed to enter the magnetic field using a range of impact angles and the particle trajectories were followed long enough to determine if the particles stay in the finite field

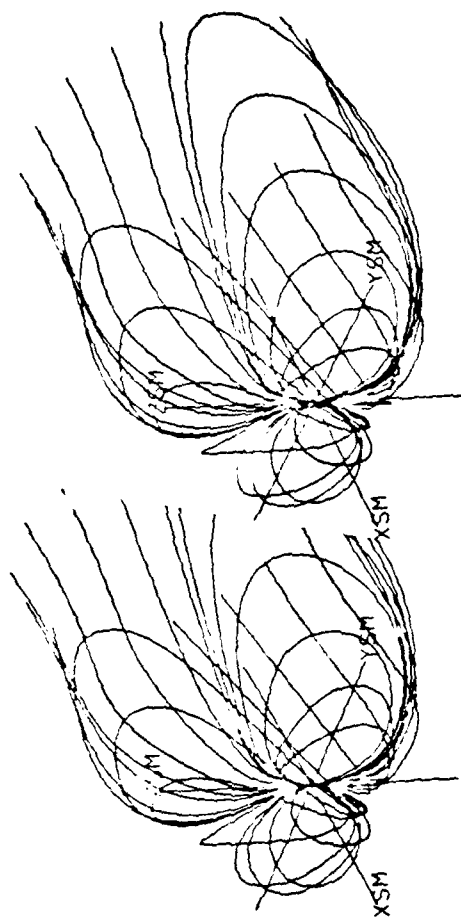


Figure 2. Stereoscopic View of Magnetic Field Lines Near the Boundary of the Magnetosphere

region. Figures 3-7 summarize the entry of 5 KeV protons at specific locations on the magnetosphere. They show a polar graph tangent to the magnetosphere at the impact point. The direction of the \bar{B} vector at the impact point determines the zero azimuth abscissa. Also shown on the graph is the projection of the X_{SM} axis onto the plane. The circles are circles of constant elevation angle (above the impact plane) for the impacting particles. Thus the point marked 90° shows a perpendicular particle impact with the surface. The zero degree curve shows particles with a zero degree elevation or a grazing impact with the boundary. The angular direction away from the \bar{B} vector gives the azimuth of the impact direction. The shaded area shows where particle entry is possible. Thus one sees that protons with low elevation angles and moving in the antisolar direction are able to enter the magnetosphere. The various figures (Figures 3-7) show how the acceptance cone changes with the X_{SM} distance and with magnetospheric location.

The entry cone curves were combined with an isotropic proton distribution and "fractional entry values" (the fraction of entering particles divided by the total incident number) were calculated as a function of energy and magnetospheric position. Figures 8 through 10 show the entry values at three different X_{SM} and three different energies plotted versus the angle above the equatorial plane (angle is the arctangent of $Z_{SM} \div (-Y_{SM})$). One notes that entry is confined to the region near the equatorial plane. Outside of the region within $15-20^\circ$ of the equator the entry efficiency is almost zero. Entry efficiency increases with increasing distance down the tail and also increases with increasing energy.

The fraction of protons able to enter into a closed magnetosphere is large. With an isotropic flux outside the boundary, 10-30% of the protons are able to enter near the magnetic equator. Since the entry cone is directed toward $+X_{SM}$ (toward the sun), the entry efficiency is even greater for particles streaming in the antisolar direction, i.e., for the magnetosheath plasma.

PROTON ENTRY INTO MAGNETOSPHERE

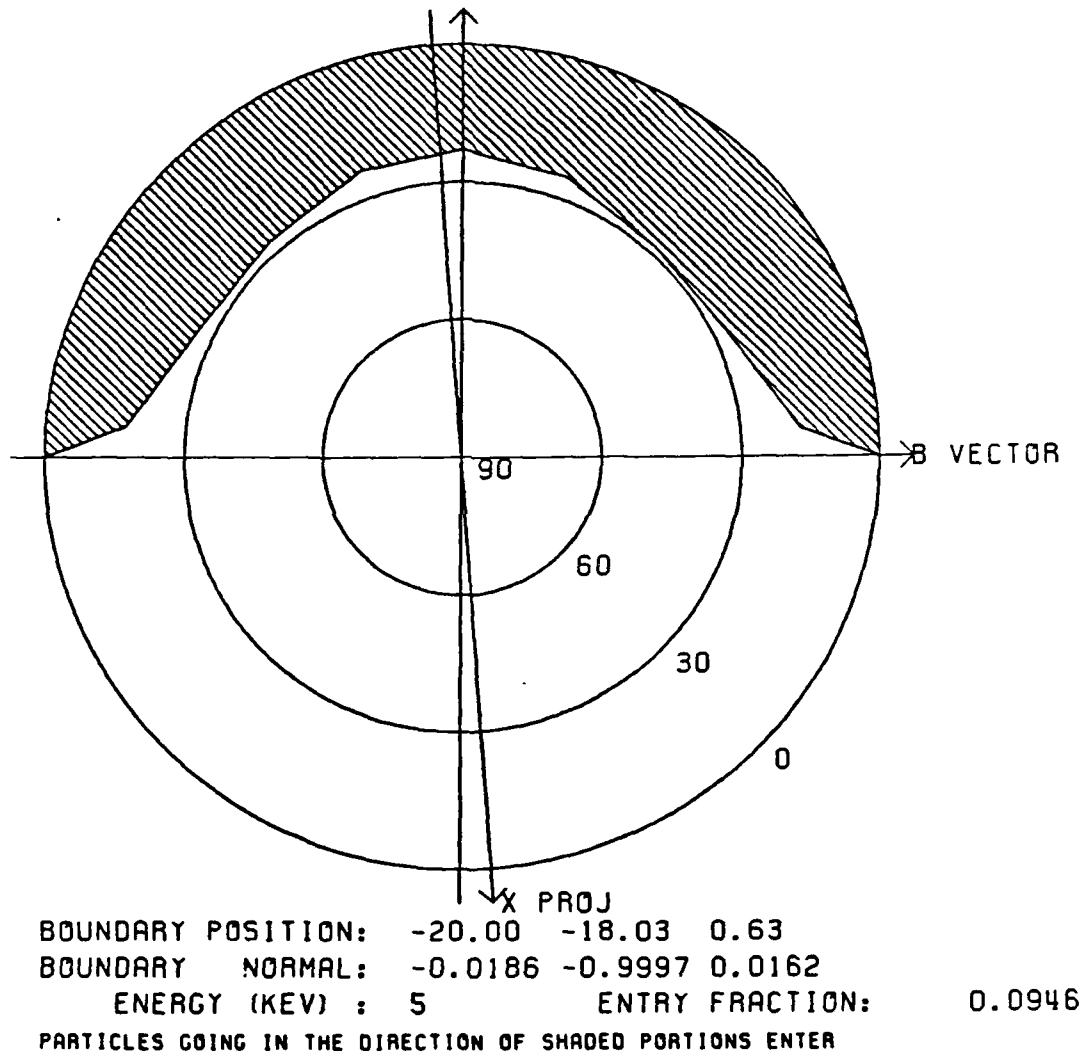
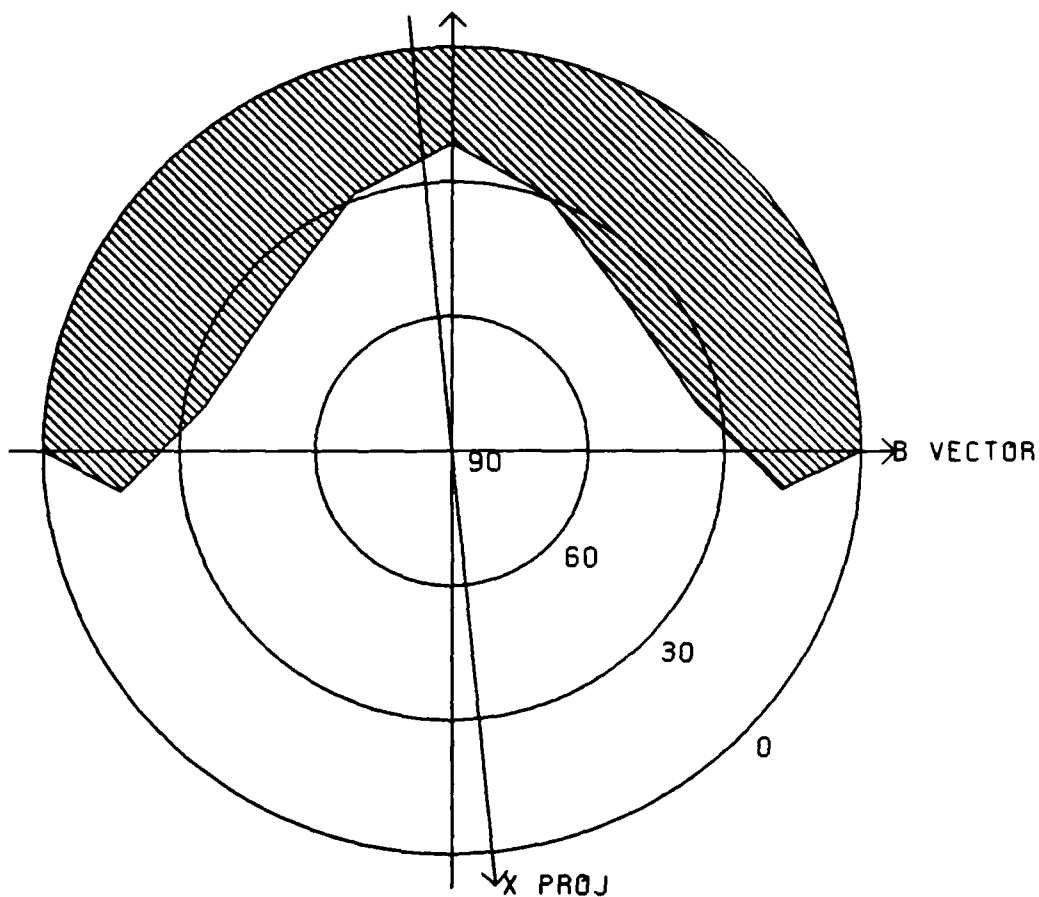


Figure 3. Proton Entry into Magnetosphere

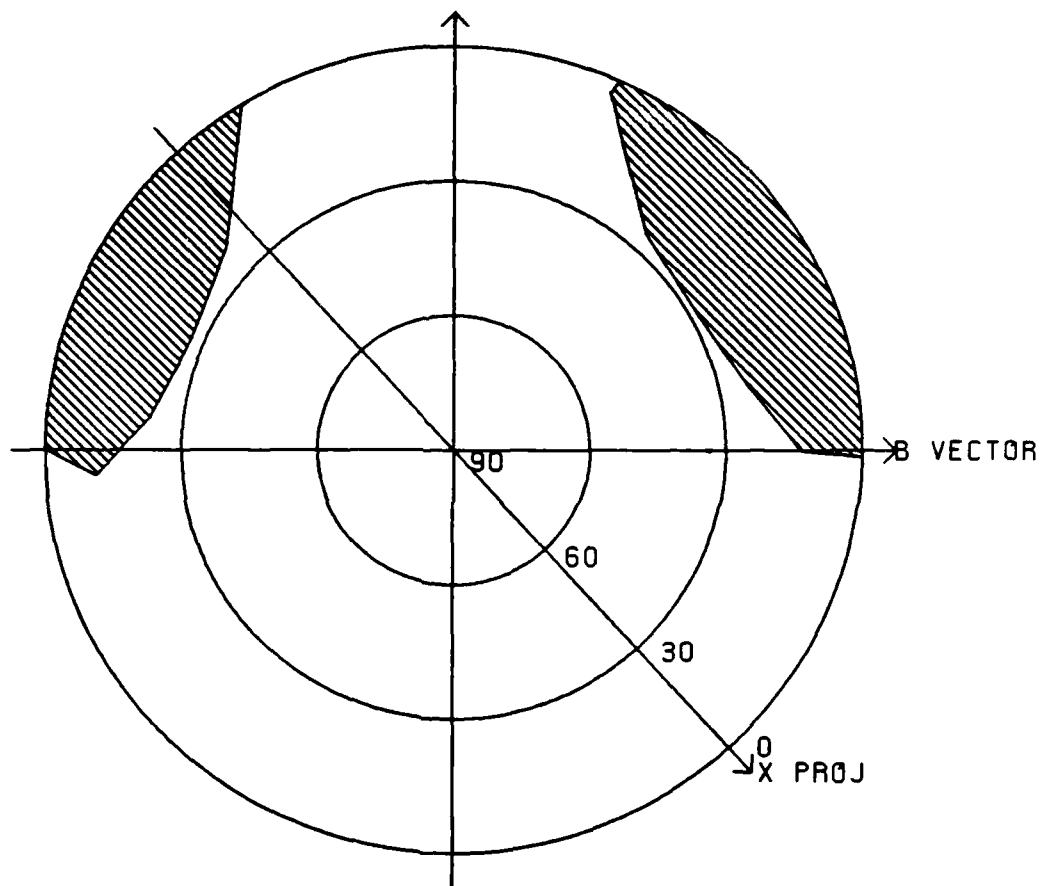
PROTON ENTRY INTO MAGNETOSPHERE



BOUNDARY POSITION: -30.00 -17.59 0.62
 BOUNDARY NORMAL: -0.0512 -0.9987 0.0084
 ENERGY (KEV) : 5 ENTRY FRACTION: 0.1641
 PARTICLES GOING IN THE DIRECTION OF SHADED PORTIONS ENTER

Figure 4. Proton Entry into Magnetosphere

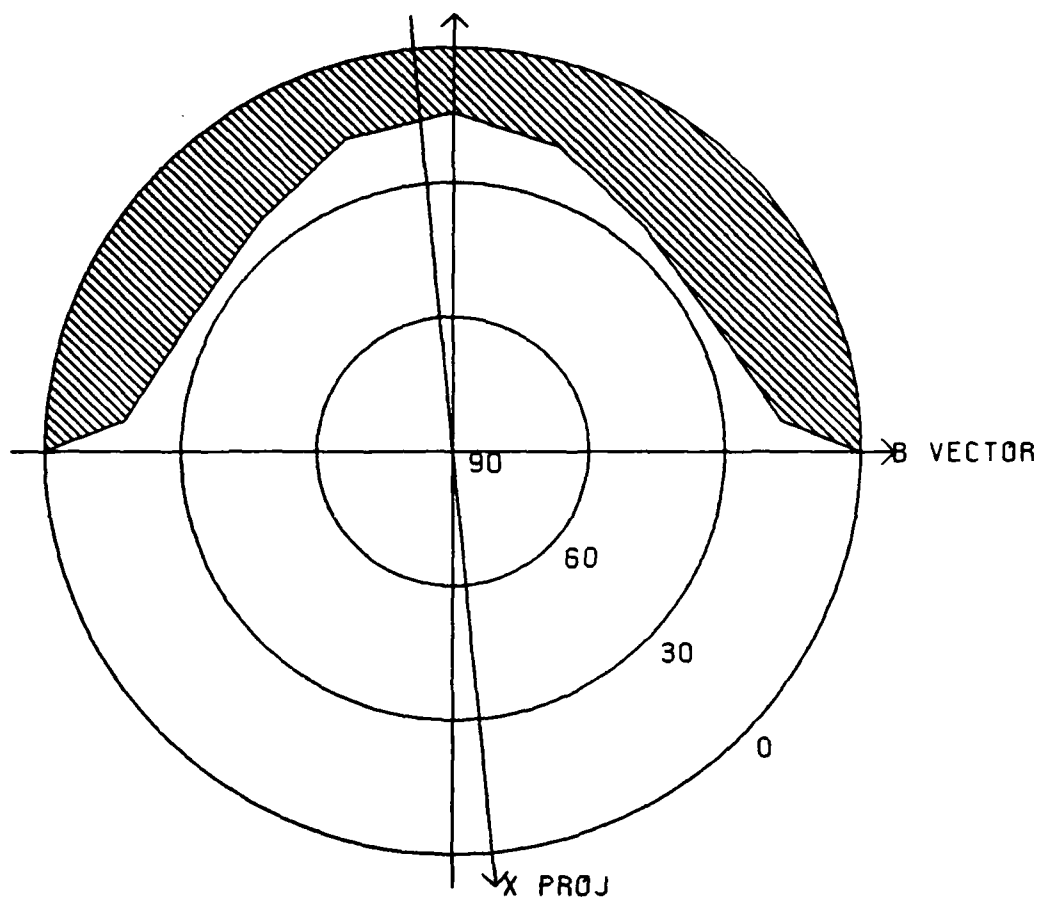
PROTON ENTRY INTO MAGNETOSPHERE



BOUNDARY POSITION: -30.00 -17.44 4.67
 BOUNDARY NORMAL: -0.0396 -0.9966 0.0717
 ENERGY (KEV) : 5 ENTRY FRACTION: 0.0572
 PARTICLES GOING IN THE DIRECTION OF SHADED PORTIONS ENTER

Figure 5. Proton Entry into Magnetosphere

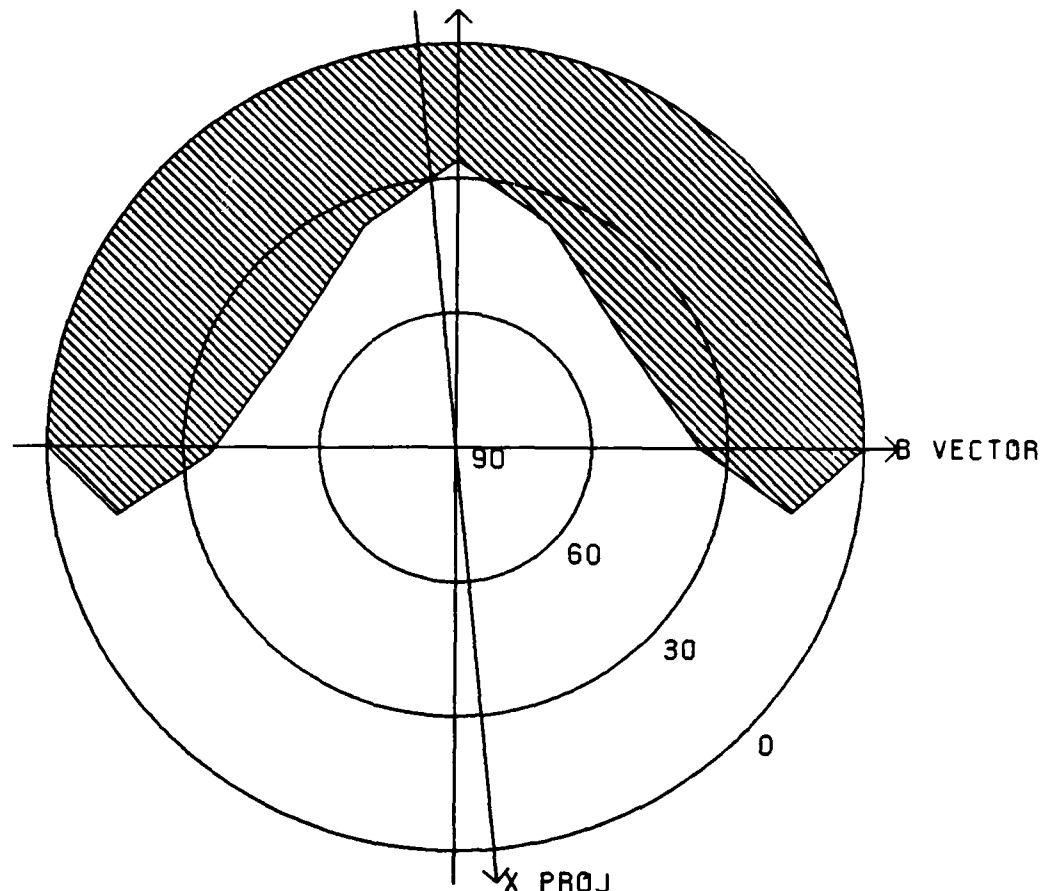
PROTON ENTRY INTO MAGNETOSPHERE



BOUNDARY POSITION: -30.00 -17.59 0.62
 BOUNDARY NORMAL: -0.0512 -0.9987 0.0084
 ENERGY (KEV) : 1 ENTRY FRACTION: 0.0718
 PARTICLES GOING IN THE DIRECTION OF SHADED PORTIONS ENTER

Figure 6. Proton Entry into Magnetosphere

PROTON ENTRY INTO MAGNETOSPHERE



BOUNDARY POSITION: -30.00 -17.59 0.62
 BOUNDARY NORMAL: -0.0512 -0.9987 0.0084
 ENERGY (KEV) : 10 ENTRY FRACTION: 0.2268
 PARTICLES GOING IN THE DIRECTION OF SHADED PORTIONS ENTER

Figure 7. Proton Entry into Magnetosphere

1 KEV PROTON

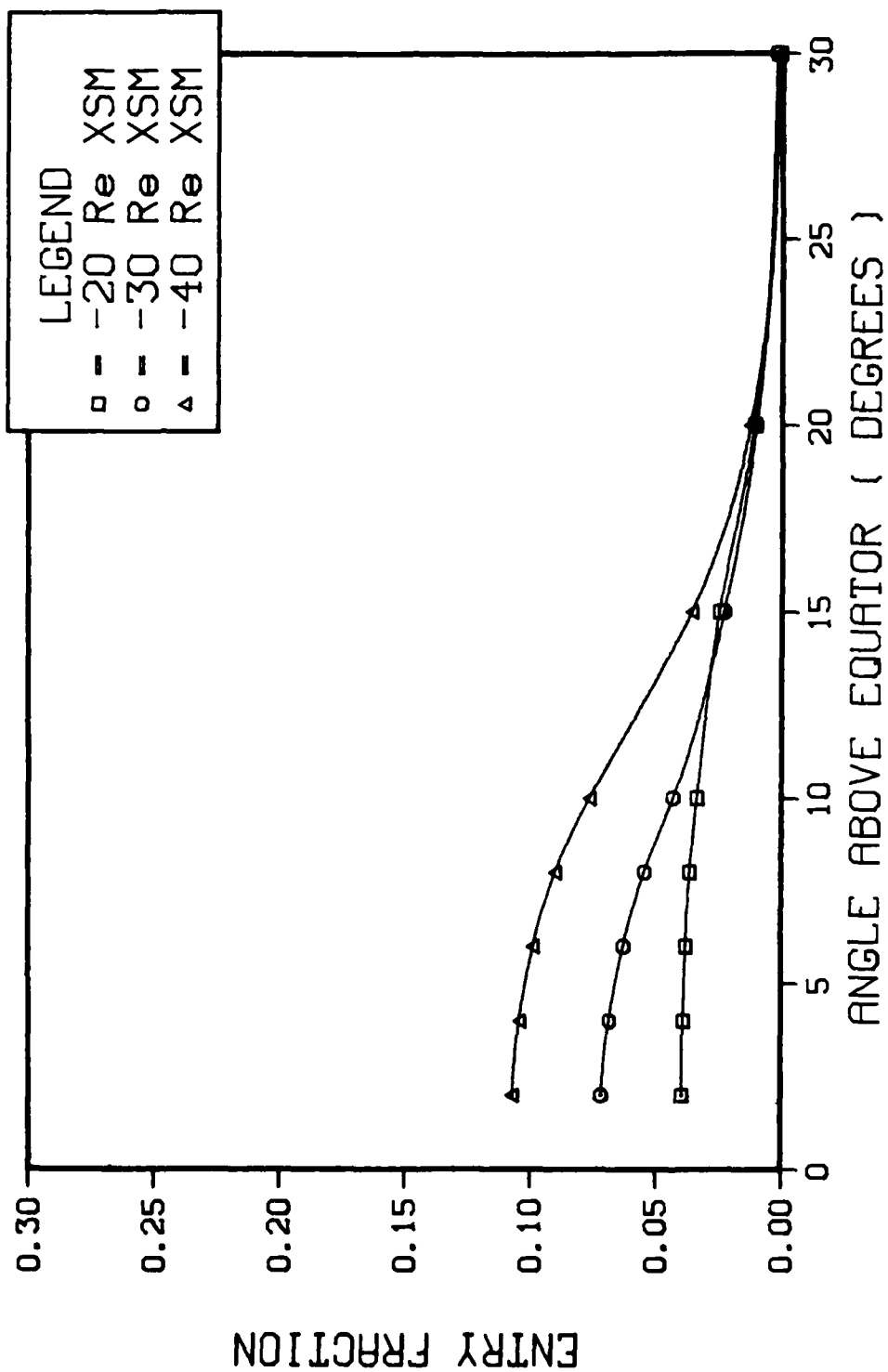


Figure 8. 1 KeV Proton

5 KEV PROTON

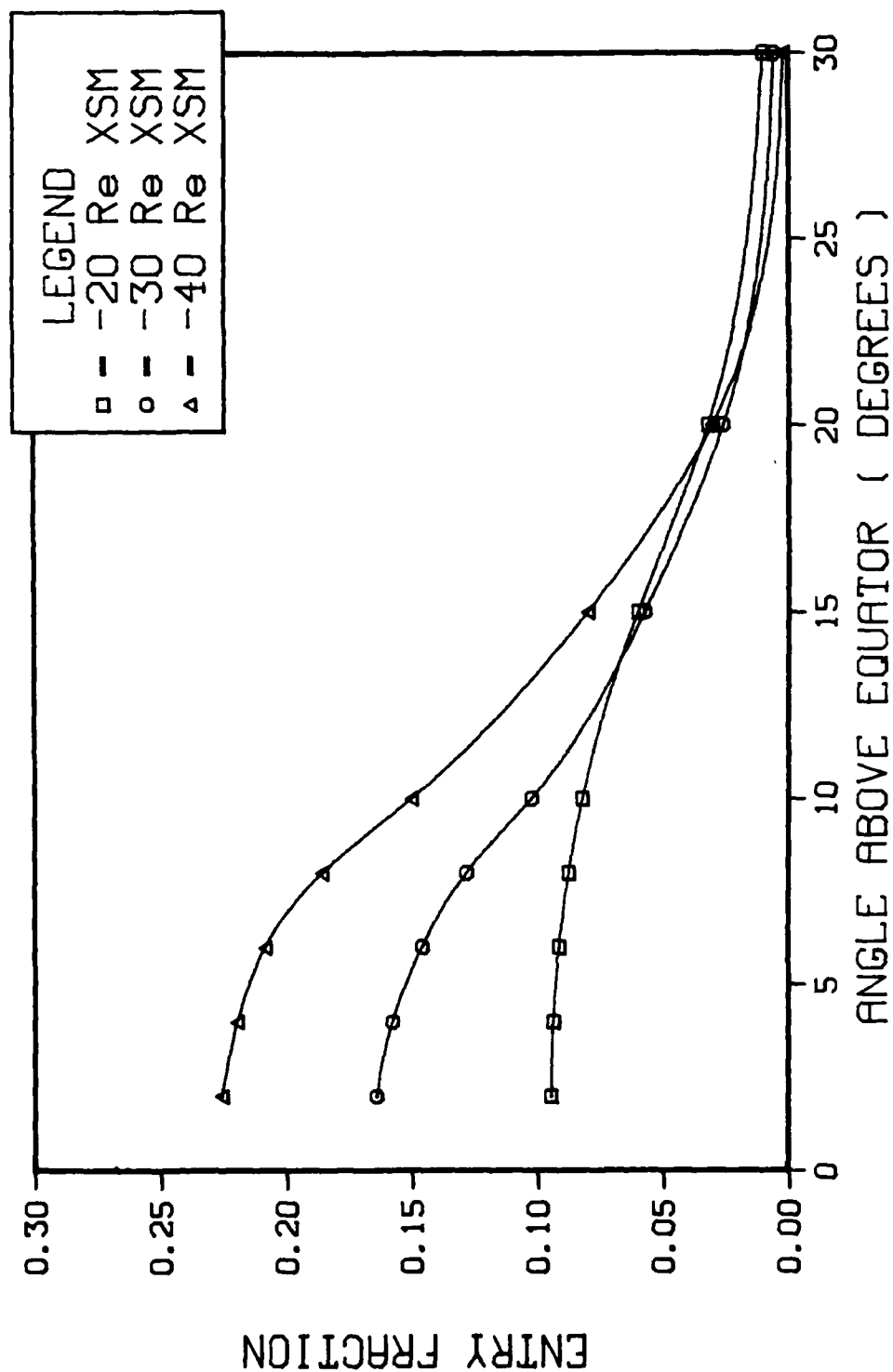


Figure 9. 5 KeV Proton

10 KEV PROTON

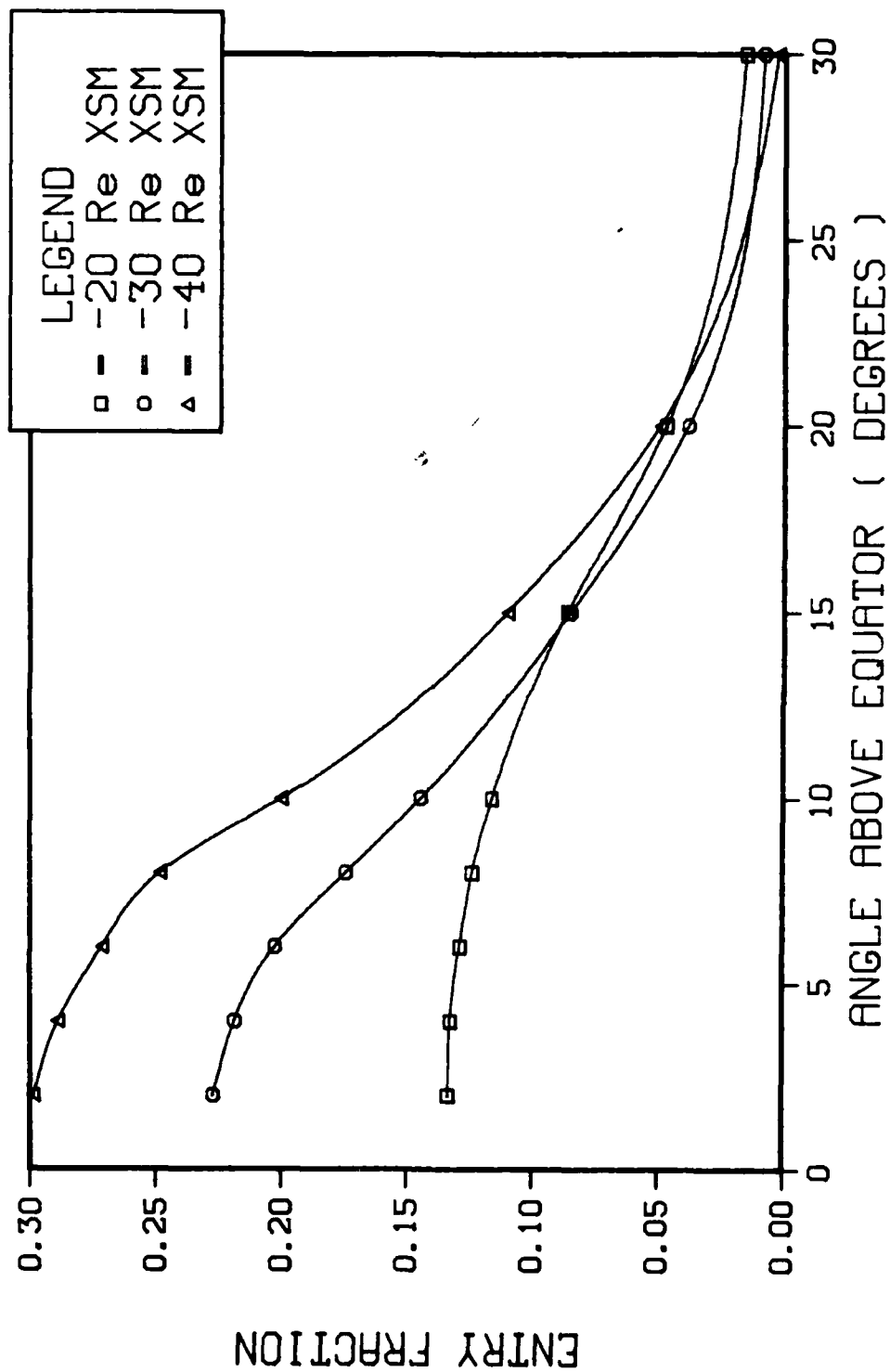


Figure 10. 10 KeV Proton

Entry efficiency increases with particle energy and thus the particle energy distribution inside and outside the boundary will be different. This energy dependent entry mechanism helps to explain the observed difference in energy spectrum between the magnetosheath and the plasma sheet. The distribution functions, however, are also dependent on particle drift velocity inside the boundary and tail and boundary fields.

The initial calculations for the magnetospheric magnetic field used specular reflection as one of the basic assumptions. The relatively large entry through the closed boundary implies that the specular reflection condition is not correct. Particles which enter the magnetosphere will have a different momentum change than specularly reflected particles. This more realistic description of particle entry will modify the predicted theoretical magnetospheric shape, predicting a slightly blunter, more flared magnetosphere. This is consistent with observations.

The calculation of entry efficiency is only a first step in understanding the tail entry mechanism, the formation of the plasma sheet, and the ultimate understanding of the substorm processes. The closed field entry mechanism permits the entry of protons on the dawn side and electrons on the dusk side. Electron entry has only been qualitatively studied. Initial results indicate that electrons have a smaller entry cone than similar energy protons.

This difference in entry efficiency will cause charge separation at the boundary and complicate the entry and transport of charged particles into and through the plasma sheet. To do the following correctly, it is clear that ideally the magnetopause shape, the formation of electrostatic fields, and magnetopause microphysics problems must all be considered self-consistently. Clearly, even with today's computer power, this is close to impossible. It is therefore our plan to first redetermine magnetopause shape by taking into account the impact of particle entry in the pressure balance formalism. We will try to ask and answer questions concerning any impact that electrostatic fields may have on this determination of magnetopause shape. With the new shape, we will then again determine charged particle entry and proceed to examine the formation of electrostatic fields and magnetopause microphysics generally.

Section 3

THE LOCAL ACCELERATION OF CHARGED PARTICLES IN THE INNER MAGNETOSPHERE

In this section we discuss our investigation of the mechanisms for trapped proton energization during quiet times. We have determined numerically the response of geosynchronous protons to the total electric and magnetic fields caused by the earth's internal dipole moving relative to an external magnetic field assuming that the ionosphere and magnetic field lines are perfect conductors (essentially, the electromagnetic field produced by the daily "wobble" of the geomagnetic dipole and the response of the magnetosphere to this motion). This study has allowed us to determine practical requirements that must be placed on field models when they are used to integrate particle motion. The biggest constraint on numerically solving for a particle's motion is the speed with which a computer model of \bar{E} will return the electrostatic potential at a point in space. Because of the assumption of perfectly conducting magnetic field lines ($\bar{E} \cdot \bar{B} = 0$) and using the decomposition of \bar{E} into a scalar and vector potential part ($\bar{E} = \frac{1}{c} \frac{\partial \bar{A}}{\partial t} - \nabla \phi$), we can say that

$$\frac{d\phi}{ds} = - \frac{\partial A_{\parallel}}{\partial t}$$

where s is distance along a magnetic field line and A_{\parallel} is the component of \bar{A} parallel to the field line. So to determine ϕ at one point in space requires an integral from a boundary along the field line to the point specified. The gradient $\nabla \phi$ requires at least four such integrals which are very time consuming for the accuracy needed. In the energization problem studied, we circumvented this great computational expense by formulating a near-earth field model using a useful mathematical tool, Euler potentials.

A review of the use of Euler potentials for magnetic field models is given by Stern (1976). Briefly, these potentials, α and β , have properties that allow us to express total \bar{B} and \bar{E} fields as point-wise functions. α and β are also constant on any given magnetic field line. This allows us to quickly map a

point in space with known α and β to a boundary point with the same α and β . Other properties important for their use in field models are summarized in Figure 11. One problem with these potentials is that \bar{B} is given nonlinearly by α and β so that it is generally difficult to determine models for α and β from given observations of \bar{B} . For our near-earth energization study, we could linearize their determination using Stern's (1967) method. This method is summarized in Figure 12.

Because of the computational advantages of using field models expressed by Euler potentials, we are investigating other ways of constructing more general models that will be valid in the magnetotail. Another property of these potentials makes them attractive for tail models; it is relatively easy to constrain all the field lines leaving the earth to stay on one side of an arbitrary surface, thus the magnetopause of a closed magnetosphere can be explicitly specified in an Euler potential field model. It is planned to exploit this in the study of particle entry (described in another section of this report).

RESULTS

The near-earth Euler potential field model described above was used with a program developed to trace the guiding center motion of a proton in a magnetic mirror geometry. The particle is assumed to conserve its magnetic moment and a zero longitudinal adiabatic invariant. It is therefore constrained to remain at the minimum B position of a field line. Field lines leaving the earth in the noon-midnight plane between 63° and 69° magnetic latitude are shown in Figures 13 and 14. Figure 13 is for the solar wind incident perpendicular to the dipole, while Figure 14 is for a 35° tilt of the dipole axis with respect to its perpendicular direction. In both figures, the compressed nose and extended tail are apparent. Thus it is apparent that the Euler potential representation of the magnetospheric magnetic field is appropriate and yields a realistic magnetic field geometry out to the region beyond geosynchronous orbit.

EULER POTENTIALS α, β

$$\bar{B} = \nabla \alpha \times \nabla \beta, \quad \bar{A} = \alpha \nabla \beta$$

$$\bar{E} = -\frac{1}{c} \frac{\partial \bar{A}}{\partial t} - \nabla \phi, \quad \text{becomes}$$

$$\bar{E} = -\frac{1}{c} \bar{W} \times \bar{B} - \nabla (\phi + \psi); \quad \text{where}$$

$$\bar{W} = \left[\frac{\partial \beta}{\partial t} \nabla \alpha - \frac{\partial \alpha}{\partial t} \nabla \beta \right] \times \frac{\bar{B}}{B^2}$$

$$\psi = \frac{1}{c} \alpha \frac{\partial \beta}{\partial t}$$

ASSUMPTION $\bar{E} \cdot \bar{B} = 0$ IMPLIES

$\phi + \psi = \text{CONSTANT ON FIELD LINE}$

Figure 11. Euler Potentials α and β

PERTURBATION METHOD OF STERN

$$\bar{B} = \bar{B}_i + \bar{B}_e ; \quad \bar{B}_i \text{ is Dipole } \bar{B}$$

$$\alpha = \alpha_i + \alpha_e ; \quad \alpha_e \ll \alpha_i \text{ (KNOWN)}$$

$$\beta = \beta_i + \beta_e ; \quad \beta_e \ll \beta_i \text{ (KNOWN)}$$

$$\bar{B}_i = \nabla \alpha_i \times \nabla \beta_i$$

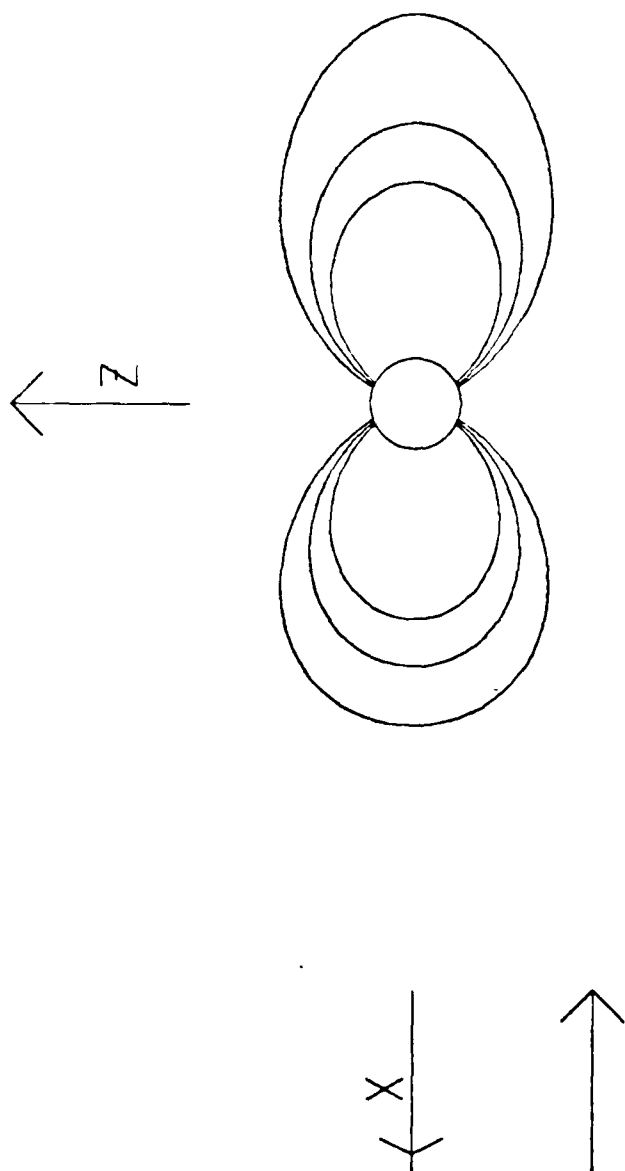
$$\bar{B}_e = \nabla \alpha_i \times \nabla \beta_e + \nabla \alpha_e \times \nabla \beta_i$$

SOLVE FOR α_e , β_e WE USE

$$\bar{B}_e = a \hat{Z}_{SMS} \hat{X}_{SMS} + (b \hat{X}_{SMS} + c) \hat{Z}_{SMS}$$

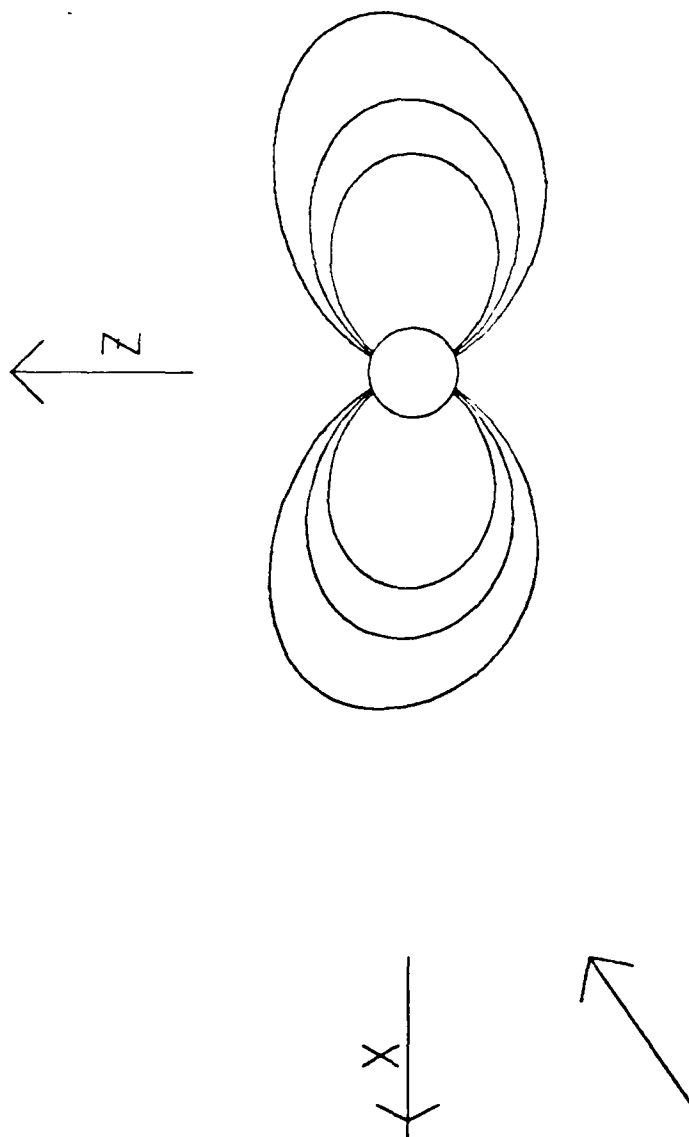
PERTURBATIONS "SMALL" AT GEOSYNCHRONOUS ORBIT

Figure 12. Perturbation Method of Stern



DEGREES TILT = 0.0
 STARTING LAT = 63.
 DEG INCREMENT = 3.
 ENDING LAT = 69. B MODEL = BESPHERE2

Figure 13. Magnetic Field Lines in the Noon-Midnight Meridian Plane



DEGREES TILT = -35.0
 STARTING LAT = 63.
 DEG INCREMENT = 3.
 ENDING LAT = 69. B MODEL = BESPHERE2

Figure 14. Magnetic Field Lines in the Noon-Midnight Meridian Plane

With the Euler potentials it is, of course, also possible to quickly obtain the induced electric field. With the induced electric field and the magnetic field topologies represented in terms of α and β . It is then possible to do the integrations required to find the total magnetospheric electric field (recall that because the Euler potentials have been used, these integrations can now essentially be avoided because the entire field line is represented by constant values of α and β). Having determined the magnetic and total electric field in the magnetosphere, we are finally in a position to study the energization of charged particles.

It has been mentioned that while appreciable energy gain is possible over several hours, the question of "phasing" a particle's position so that it will gain energy over more prolonged periods must be answered. This question is more complicated than only trying to be at the right position at the right time. To answer this question we note first that, as shown in Figure 11, the electric field has parts $(-\nabla(\frac{1}{2} + \dots))$ and $(-\frac{1}{c} \bar{W} \times \bar{B})$ that can contribute to energization. The first term is completely independent of the earth boundary condition. However, this part (together with the assumed analytic boundary condition of a uniformly magnetized rotating charged conducting sphere) will always cause energization of protons on the dawn side and de-energization on the dusk side of the earth. But, because it is due to the gradient of a potential, its net contribution to energization after one particle orbit is nil. The second term is due to the time dependence of the fields and can produce a net change in particle energy over a complete orbit. It is for this part that phasing is important.

We note in passing that use of the Euler potentials has allowed us to separate out that portion of the electric field which depends on the earth boundary condition. The remaining portion of the electric field contains the time dependence and is responsible for the non-conservative portion of the total electric field. Thus the use of Euler potentials makes our study of permanent particle energization much more amenable.

The phasing needed to gain energy from the non-conservative part of \bar{E} can be determined from Figure 15. The \bar{E} field values shown are for points on the sun-earth line that intersect a typical particle's orbit at zero tilt. The field shown in the direction of particle drift so that positive values cause energization and negative values cause de-energization. Three conclusions are apparent from this figure: (1) the electric field is controlled by the tilt; (2) the particle will gain (or lose) more energy on the day side than on the night side; and, (3) a particle with a half-day drift period that is correctly phased (i.e., starts at the nose position at zero time for Figure 15) will always gain energy from the conservative part of \bar{E} .

Integrations of particle guiding centers over several days are shown in Figures 16 through 21. All particles started out at the same position in the nose and were initially phased to gain energy from the non-conservative part of \bar{E} . In all these figures a high frequency oscillation about 4 KeV peak to peak is present; this is due to potential position of \bar{E} (and therefore the boundary condition). Each peak corresponds to the extreme tailward position and each valley to the sunward position of an orbit. The net energization per orbit is best seen by looking at the valleys in these figures. The initial phase allows easy interpretation of the nonpotential energy change. Whenever the particle in a valley (at the sunward position) is also at a half-day mark, the particle will be energized during the coming orbit.

The seemingly random pattern in Figure 16 is explained by the above remarks. The drift period for the 11 KeV proton is too long to stay in phase with the tilt very long. The 12 KeV proton (Figure 17) initially has a drift longer than half-day, but close enough to gain energy and remain in phase by decreasing the drift period for two days. The particle is then phased to lose energy until day 5. What looks like a complete cycle has occurred at day 5.5. Figure 18 shows behavior similar to Figure 17; the superposition of high and low frequency waves. The 15 KeV proton (Figure 19) is quickly caught in a phasing where it will continue to lose energy. The particle integration was stopped when the proton exited what we considered the valid spatial region of the field model. Because of the cyclical behavior of the previous cases, it is assumed that it would be possible to energize a particle

TYPICAL ENERGIZATION PARAMETERS

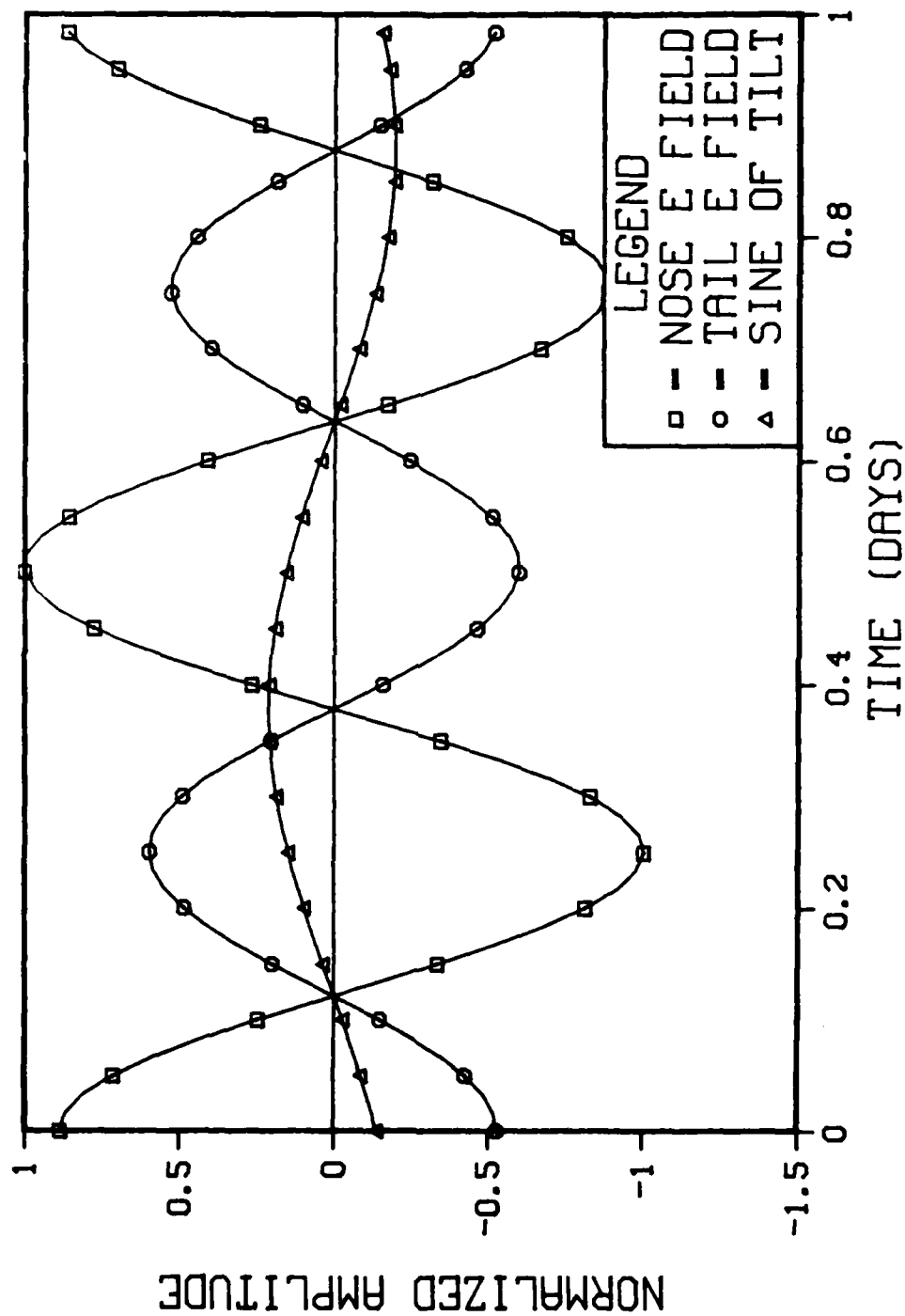


Figure 15. Typical Energization Parameters

QUIET TIME PROTON ENERGIZATION

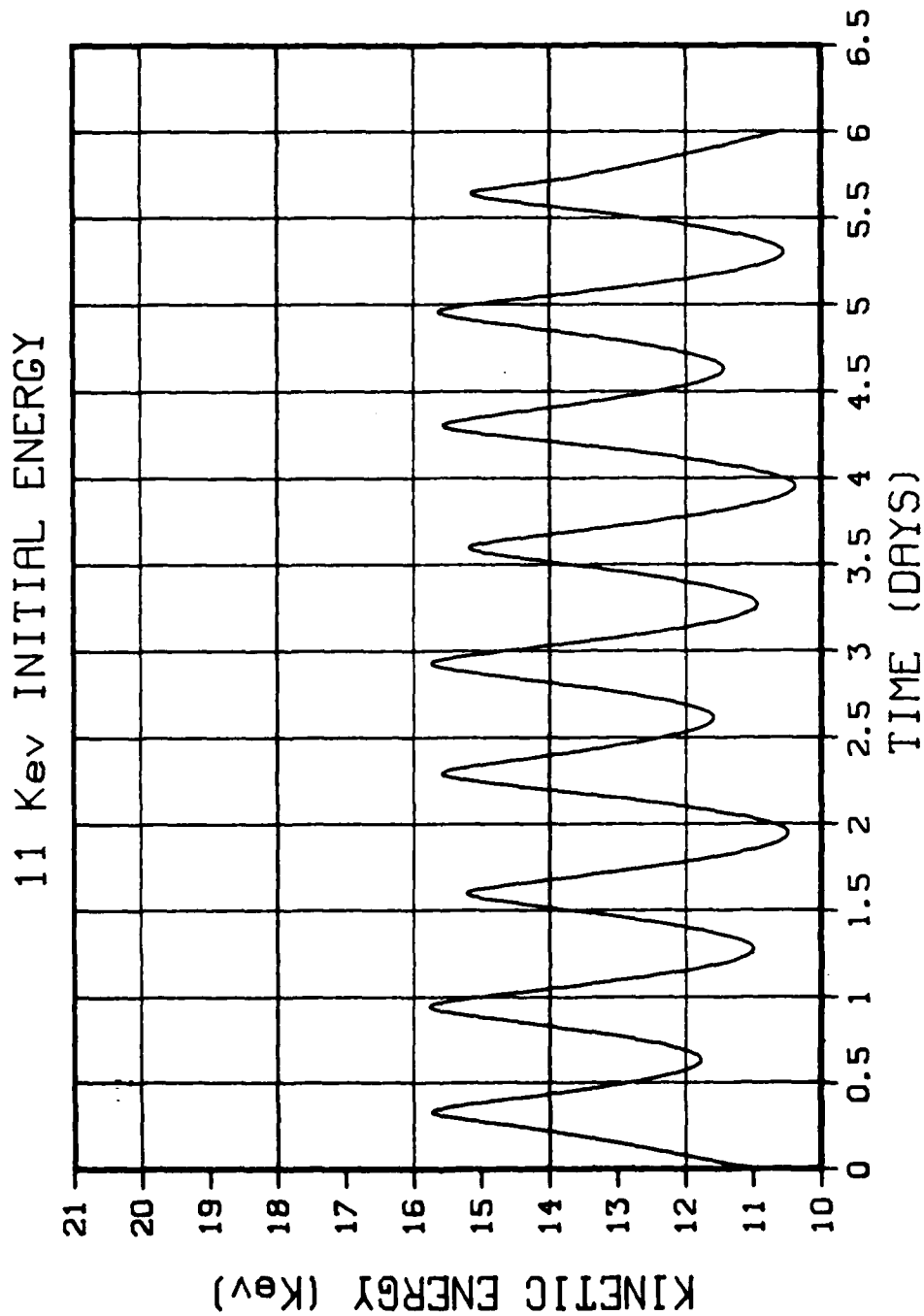


Figure 16. Quiet Time Proton Energization

QUIET TIME PROTON ENERGIZATION

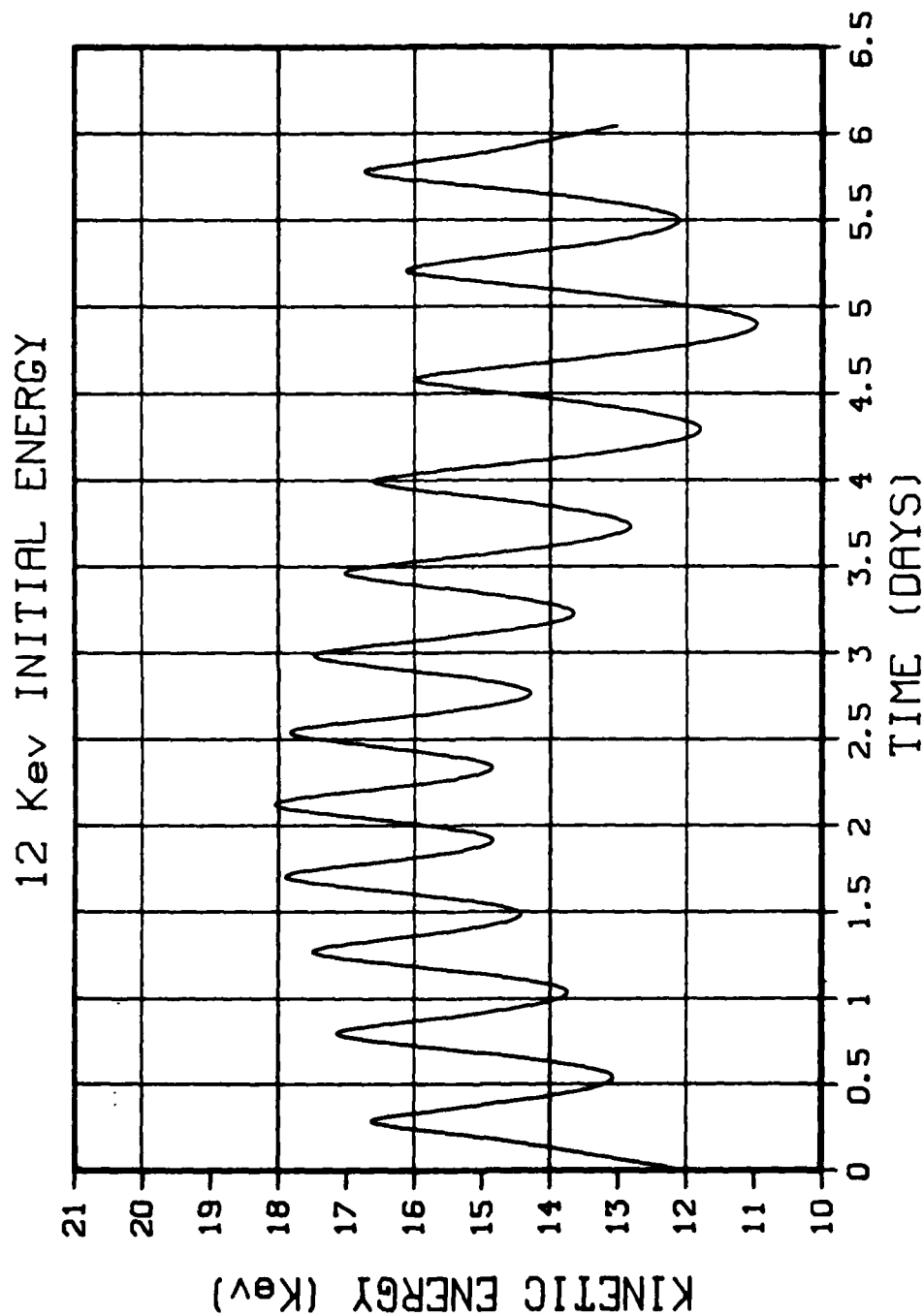


Figure 17. Quiet Time Proton Energization

QUIET TIME PROTON ENERGIZATION

13 Kev INITIAL ENERGY

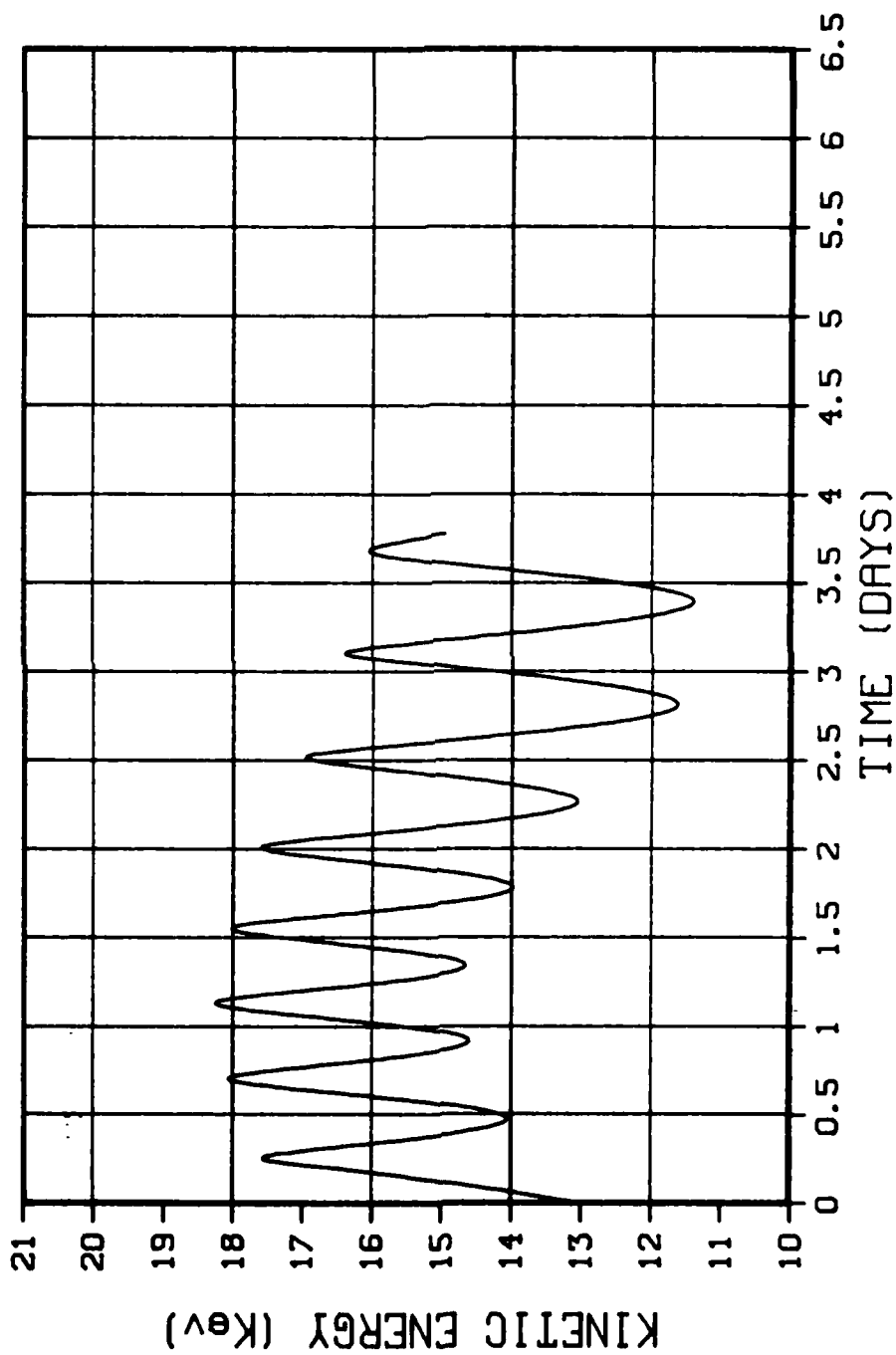


Figure 18. Quiet Time Proton Energization

QUIET TIME PROTON ENERGIZATION

15 KeV INITIAL ENERGY

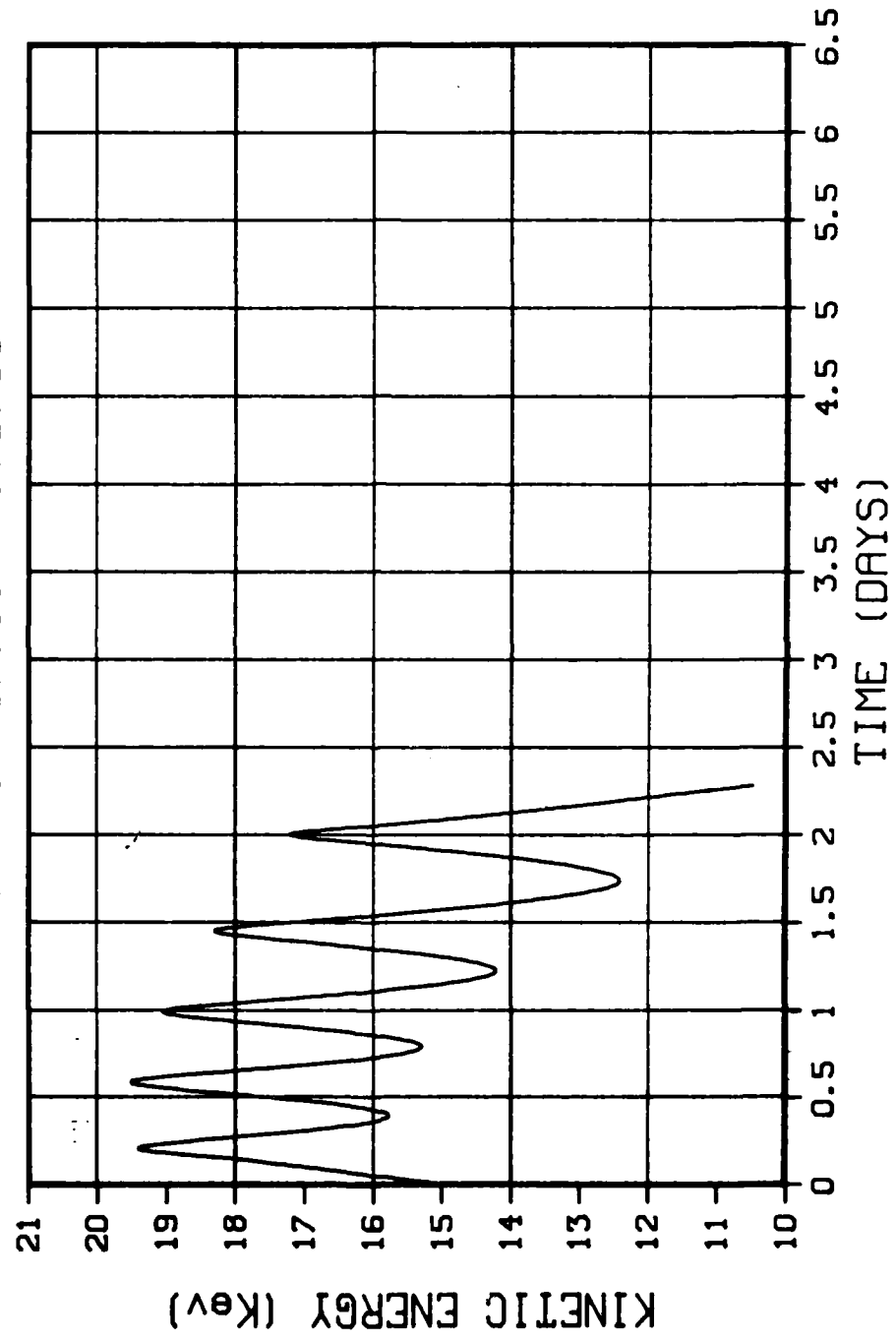


Figure 19. Quiet Time Proton Energization

QUIET TIME PROTON ENERGIZATION

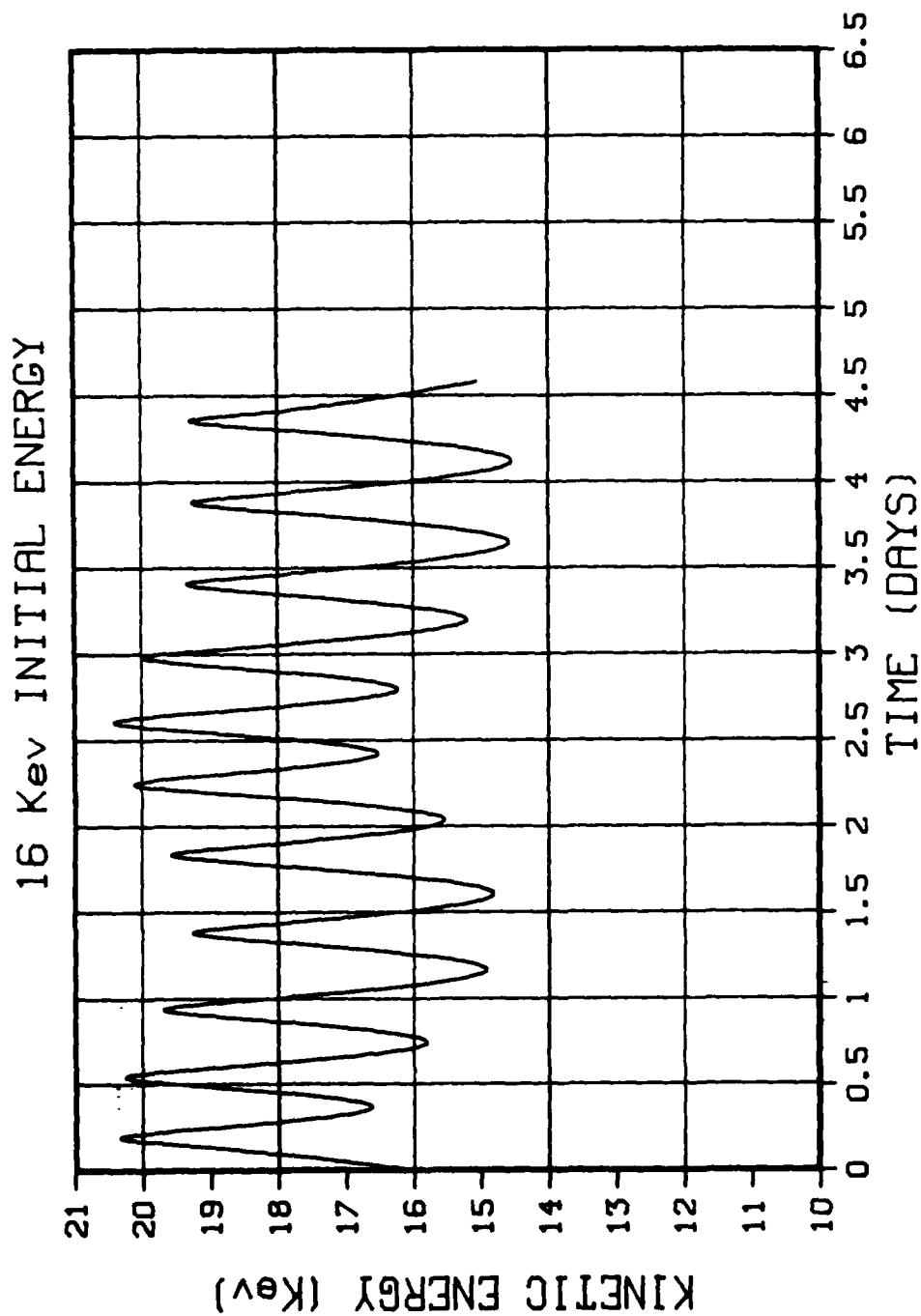


Figure 20. Quiet Time Proton Energization

QUIET TIME PROTON ENERGIZATION

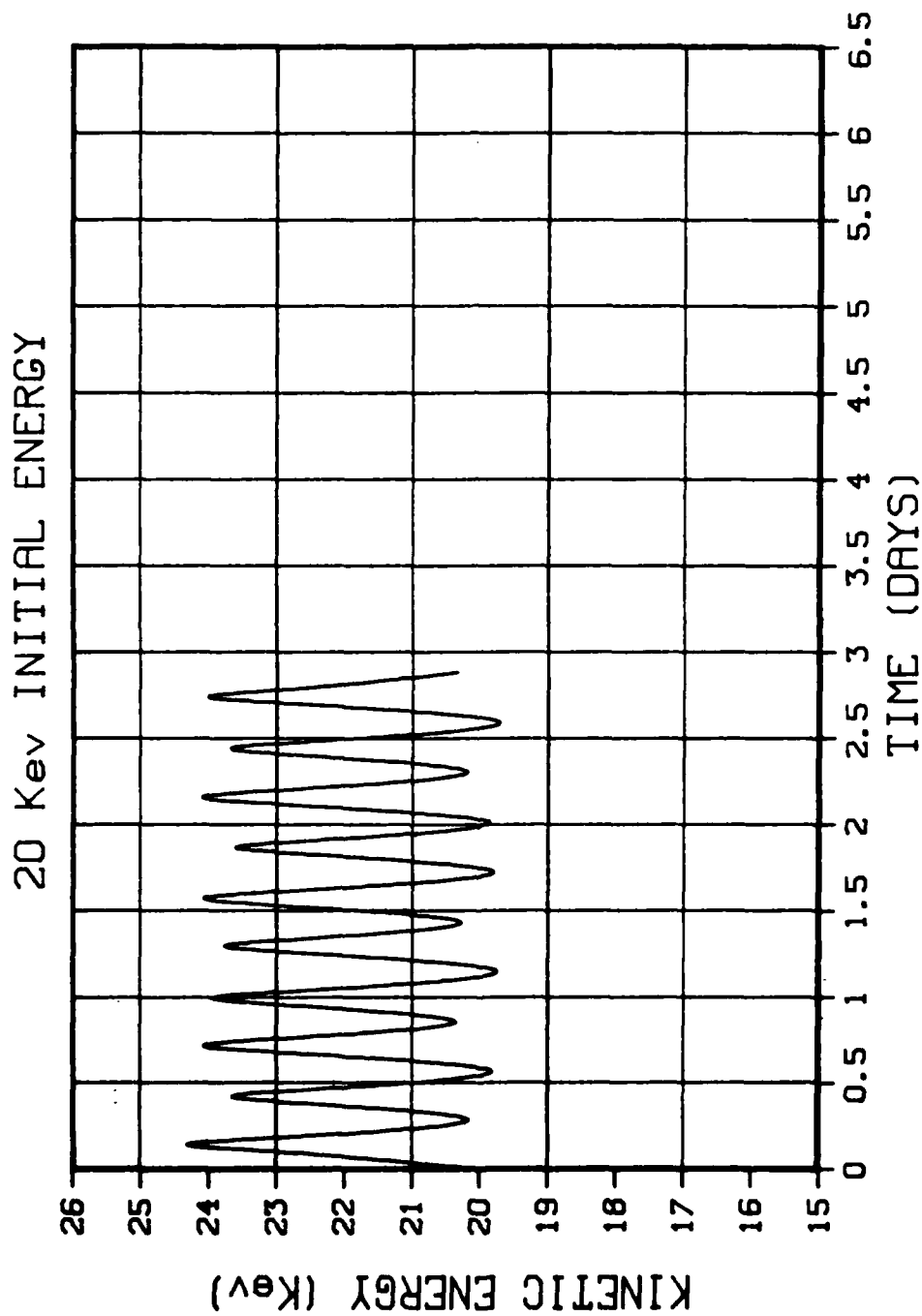


Figure 21. Quiet Time Proton Energization

near the limit of the model's valid region by the same magnitude as Figure 19 shows de-energization. The 16 KeV case (Figure 20) is much better behaved and we see the effect of non-conservative \bar{E} energization becoming smaller as the drift period decreases. The 20 KeV proton (Figure 21) seems just as random as the 11 KeV case; once again, the cause determined by phasing.

There are two distinct quiet time energization mechanisms due to conservative and non-conservative \bar{E} . The conservative part of \bar{E} (which can be represented as a scalar potential) is caused primarily by the earth boundary condition and synchronized with local time. It contributes about 4 KeV to the energy variability of particles near geosynchronous orbit. The nonpotential \bar{E} is caused by time-dependent field topology alone. It is synchronized with the dipole tilt and has its larger effect on the sunward side of the earth. Particles that are phased correctly and keep a half-day drift period can have a net change of about 6 KeV over two days of orbits as was seen in the 16 KeV initial energy case.

Section 4

LIST OF PRESENTATIONS AND PUBLICATIONS

1. Olson, W. P. Accuracy of Magnetic Field Models in the Vicinity of the Earth. EOS, Trans. AGU, 62, 268, 1981.
2. Pfitzer, K. A., S. J. Scotti, W. P. Olson. Particle Entry into a Magnetically Closed Magnetosphere. EOS, Trans. AGU, 62, 370-371, 1981.
3. Scotti, S. J., K. A. Pfitzer, W. P. Olson. Quiet Time Trapped Proton Energization. EOS, Trans. AGU, 62, 361, 1981.
4. Olson, W. P., S. J. Scotti, K. A. Pfitzer. The Acceleration of Charged Particles by the Daily Wobble of the Geomagnetic Field. To be presented at IAGA, Edinburgh, Scotland, August 1981.
5. Olson, W. P., K. A. Pfitzer. The Quantitative Representation of the Magnetospheric Electromagnetic Field for Specific Events. To be presented at IAGA, Edinburgh, Scotland, August 1981.
6. Pfitzer, K. A., W. P. Olson. Quantitative Magnetospheric Studies Using Magnetic and Electric Field Models. To be presented at IAGA, Edinburgh, Scotland, August 1981.
7. Pfitzer, K. A., W. P. Olson. The Contribution of Non-Ionospheric Currents to Variations in the Earth's Surface Magnetic Field. To be presented at IAGA, Edinburgh, Scotland, August 1981.

REPORT DOCUMENTATION PAGE		READ INSTRUCTIONS BEFORE COMPLETING FORM
1. REPORT NUMBER	2. GOVT ACCESSION NO. AD-A202 550	3. RECIPIENT'S CATALOG NUMBER
4. TITLE (and Subtitle) Electric Fields in Earth Orbital Space		5. TYPE OF REPORT & PERIOD COVERED Final Report
7. AUTHOR(s) W. P. Olson K. A. Pfitzer S. J. Scotti		6. PERFORMING ORG. REPORT NUMBER MDC-G9609
9. PERFORMING ORGANIZATION NAME AND ADDRESS McDonnell Douglas Astronautics Company 5301 Bolsa Avenue Huntington Beach, CA 92647		8. CONTRACT OR GRANT NUMBER(s) N00014-80-C-0796
11. CONTROLLING OFFICE NAME AND ADDRESS Office of Naval Research Washington, D.C. 20350		10. PROGRAM ELEMENT, PROJECT, TASK AREA & WORK UNIT NUMBERS W8QA2001
14. MONITORING AGENCY NAME & ADDRESS (if different from Controlling Office)		12. REPORT DATE June 1981
		13. NUMBER OF PAGES 34
		15. SECURITY CLASS. (of this report) Unclassified
		15a. DECLASSIFICATION DOWNGRADING SCHEDULE
16. DISTRIBUTION STATEMENT (of this Report)		
17. DISTRIBUTION STATEMENT (of the abstract entered in Block 20, if different from Report)		
18. SUPPLEMENTARY NOTES		
19. KEY WORDS (Continue on reverse side if necessary and identify by block number) induced electric fields magnetosphere pressure balance particle energization electrostatic fields		
20. ABSTRACT (Continue on reverse side if necessary and identify by block number) The formalism of pressure balance is reexamined without the assumption of specular reflection. In a realistic (non uniform) magnetic field topology a significant fraction of particles incident on the magnetopause gain access to the magnetosphere. This is especially true on the flanks of the tail. Entering particles must make a significant contribution to the plasma sheet. Particle energization in the inner magnetosphere caused by the daily wobble of the geomagnetic dipole and the magnetospheric response was also quantitatively examined. Particles with initial energies		

#20. near 10 keV can gain up to 6 keV energy over a period of a few days.

LMED
-8